

The effect of coarse particles on the microstructural evolution of porous alumina sintered at 1375 °C

S.A. Schmidt, I. Nettleship*

Department of Materials Science and Engineering, University of Pittsburgh, PA 15261, USA

Received 27 May 2003; received in revised form 15 August 2003; accepted 6 September 2003

Abstract

The objective of this study was to provide quantitative information concerning the microstructural evolution of porous alumina derived from mixtures of a fine, active powder and a coarse powder with a wide size distribution. The coarse powder increased the green density and reduced the densification rate as expected. The addition of the coarse powder also increased the average grain and pore intercepts at any particular density. However, it was concluded that coarsening of the fine powder was not affected by 30% coarse powder when sintering time was considered rather than density. Coarsening did affect the average grain size when a higher fraction of the fine powder particles were in contact with the larger particles. This is expected to be particularly important for cases where coarse particles are bonded by a relatively small fraction of fine particles of the same phase.

© 2003 Elsevier Ltd. All rights reserved.

Keywords: Al₂O₃; Coarsening; Microstructure-final; Porosity; Sintering

1. Introduction

The effect of the particle size distribution on the sintering of ceramics depends on how the particle size distribution is changed. Some studies have examined the effect of changing the standard deviation of the particle size distribution while keeping the median particle size constant. Within the practical limits of experimentation it has been found that wider particle size distributions lead to faster densification rates in intermediate stage sintering.^{1,2} However, a narrower distribution may prolong intermediate stage sintering and result in less coarsening in the final stage.³ There is relatively little quantitative information concerning the effect of particle size distribution on microstructural evolution, although modeling has predicted a significant increase in coarsening for wider distributions,⁴ to the extent that densification is significantly retarded.

The mixing of coarse and relatively fine ceramic powders has been used to control firing shrinkage for a very long time. It is well known that mixtures of this type can increase the green density although the increase is often

less than the theoretical prediction.⁵ For ceramics the less desirable result of mixing is a pronounced change in the sintering kinetics.^{6,7} The addition of fine particles in volume fractions greater than about 30 vol.% reduces the green density and enhances the densification. In contrast, the addition of a coarse fraction will reduce the densification kinetics and often results in a lower final density.

The effect of coarse particles on microstructural evolution has been studied in a qualitative way. Smith and Messing⁷ observed coarsening of the fine particles but not the coarse particles when bimodal alumina powders were sintered at 1600 °C. There has been a large amount of literature published on the effect of coarse particulates on the densification of ceramics. Initial models predicted large retardations on the densification of the fine particles due to stresses set up by a low fraction of coarse particles,⁸ although the stresses were later shown to be too low to significantly effect densification.⁹ The large particles can also cause microstructural changes. Several experimental studies have qualitatively observed spatial heterogeneity^{10–13} and suggested that networks of coarse particles are the origin of the retardation of densification of a fine grained matrix. This is often manifested as porous regions that do not densify and

* Corresponding author.

E-mail address: nettles@pitt.edu (I. Nettleship).

large crack-like voids. The prediction of crack-like voids had been made previously.¹⁴ Similar observations have been made for alumina when coarser fractions of alumina powder down to 3 μm in size were added to a 0.5 μm matrix powder.¹⁵ It is pertinent to this work to point out that the important observations contained in the studies mentioned above were not accompanied by quantitative microstructural information. However, one study by Fan and Rahman,¹⁶ conducted a quantitative examination of the microstructural evolution in a fine grained matrix phase in the presence of coarse particles of another phase. They showed that for constant heating rate sintering of a ZnO matrix containing ZrO₂ inclusions the ZrO₂ did not result in any significant coarsening of the matrix phase. In isothermal sintering slow coarsening of the matrix occurred when the densification in the matrix became very slow above 80%. They concluded that the main factors that controlled densification were the interactions between the large particles and the packing of the matrix particles around the inclusions which can lead to local differential sintering.

More recently, coarse powders with a wide particle size distribution (to give higher green density and higher creep resistance) bonded by much finer powders have been used to suppress densification in porous ceramic matrices designed for ceramic-ceramic composites.¹⁷ Since mixtures of coarse and fine powders of the same phase may be expected to coarsen, large particles of mullite were bonded with alumina. Unfortunately, silicate phases such as mullite can lead to decomposition, liquid phases and higher creep rate.¹⁸ Therefore some studies have considered using alumina matrices without mullite¹⁹ due to silica volatility under combustion conditions. It is therefore instructive to examine the extent to which mixtures of fine and coarse particles of alumina coarsen at comparatively low temperature with a view to using them as porous matrices in ceramic-ceramic composites. With this in mind the objective of this study was to determine quantitatively the effect of fine powder additions on densification and more importantly on the general microstructure development of porous alumina derived from a coarse powder with a wide size distribution. In this respect this does not represent a series of experiments on a model bimodal particle size distribution.

2. Experimental

Two alumina powders were used for the experiments. Powder P was Premalox 10 and powder A was A17-SG, both powders were supplied by Alcoa, Pittsburgh USA. First powder P was dispersed in de-ionized water with an ammonium polyacrylate dispersant (Darvan C, Vanderbilt & Co, Norwalk, Connecticut, USA) and milled with zirconia ball for 24 h. The particle size

distribution is shown in Fig. 1. The powder was then dried and weighed prior to adding the correct amount of powder A, whose particle size distribution is also shown in Fig. 1. It can be seen that powder A has a wide particle size distribution extending up to 7 μm and was not expected to densify much by itself at the sintering temperature. Extrapolation of the distribution of powder A to smaller sizes suggests that less than 10% of powder A extended into the size range of powder P. The mixture was redispersed in de-ionized water and mixed using a high power ultrasonic horn for 15 min and finally dried while being stirred to prevent segregation. The resulting granulated powders were uniaxially pressed into 12.5 mm diameter pellets and the green density was calculated from their weight and dimensions. Finally the samples were fired at 1375 °C at different times ranging from 0.2 to 30 h.

The solid volume fraction of the fired samples were determined by the Archimedes method and then the samples were sectioned, ground, polished and thermally etched at 1325 °C for 30 min. The etching treatment did not change the solid volume fraction of the samples, which was tested once again before observation of the sections using a scanning electron microscope (Philips XL-30). The volume fraction of solid, V_{vs} was determined by the standard manual point counting technique. At least 460 points were counted on each micrograph and seven micrographs were used. For each specimen a 95% confidence interval was calculated. The high magnification required for reliable imaging of the fine particles sometimes caused the 95% confidence interval for the mixtures to be larger due to the variability between the images containing large particles. With only a few exceptions the results of the Archimedes determinations fell within the 95% confidence interval of the stereological measurement suggesting that the images were collectively representative of the microstructure, at least in terms of the volume fraction of phases. The surface area density of solid–solid S_{v}^{ss} and solid–vapor boundaries S_{v}^{sv} were measured using the intercept method. In this case the intercepts were counted on orthogonal sets of equispaced lines. This

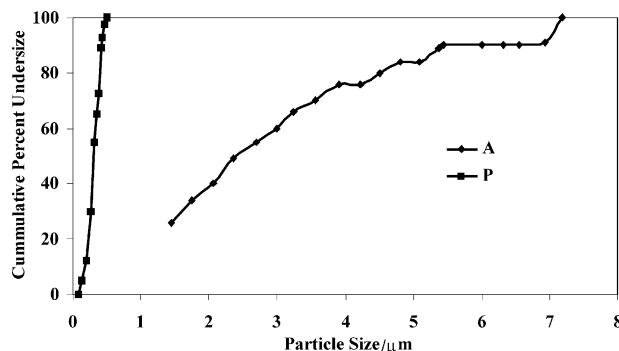


Fig. 1. A comparison of the particle size distributions of powder A and powder P.

was done on seven different images resulting in at least 1400 intercepts for each sample. The 95% confidence interval was calculated for each determination.

The mean linear pore intercept length, λ_p was calculated using:

$$\lambda_p = 4(1 - V_{vs})/S_v^{sv} \quad (1)$$

The mean linear grain intercept length λ_g was calculated assuming that all the pores were located on the grain boundaries. It was rare to see pores in the grains even at the higher densities:

$$\lambda_g = 4V_{vs}/(S_v^{sv} + 2S_v^{ss}) \quad (2)$$

The microstructural study was confined to the samples containing no more than 50% of the coarse powder because of a decision to reject solid volume fractions below 0.7 for microstructure analysis. At higher porosities it becomes difficult to extract quantitative information from images produced by imaging techniques like SEM that have a high depth of field. Also the bonding between the particles in samples with more than 50% coarse particles was not sufficiently strong to avoid pull-out during grinding and polishing of some of the samples. This caused the solid volume fraction determined by image analysis to be significantly less than that determined by the Archimedes method and therefore the samples are not suitable for further examination.

3. Results

The addition of the coarse powder widened the particle size distribution by skewing it to larger sizes rather than creating a bimodal distribution. This reflects the particle size distributions chosen for porous matrix ceramic composites in which fine alumina powder was added to a relatively coarse mullite powder with a wider particle size distribution.¹⁷ The mixtures resulted in

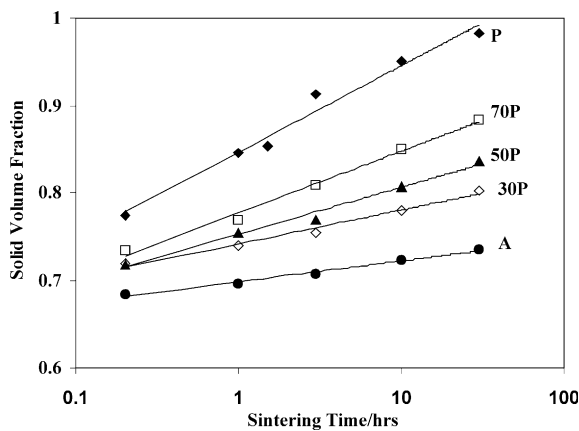


Fig. 2. The effect of the fraction of powder A on densification. The lines represent semi-log fits to the experimental results.

higher green densities with values ranging from 57% for pure P to 67% for 30%P. Fig. 2 summarizes the effects of the mixing on densification, which were much as expected. The figure includes the logarithmic fit commonly applied to ceramic sintering data for which the Pearson's correlation coefficients were all above 0.97. The addition of the coarse powder lowered the densification rate and had a pronounced effect on the sintered solid volume fraction at any particular sintering time. For example at 30 h, the longest sintering time used, the solid volume fraction decreased from 0.98 for pure P through 0.88 for 70%P to 0.84, 0.8 and 0.73 for 50%P, 30%P and pure A, respectively.

In terms of the microstructure, the effect of the powder mixing on the surface area density of solid–solid boundary is shown in Fig. 3(a). The curve for pure P is similar to the results of previous studies,²⁰ for which the value of S_v^{ss} remains roughly constant through most of intermediate sintering and then decreases in final stage sintering due to grain growth. The main effect of the coarse powder addition is to lower the value of S_v^{ss} corresponding to the plateau in intermediate stage sintering. For pure P the plateau value is approximately $4 \mu\text{m}^{-1}$ but decreases to $2 \mu\text{m}^{-1}$ for 70%P and $1 \mu\text{m}^{-1}$ for 50P. Note that the 95% confidence intervals of the solid volume fraction determinations for some of the mixtures are larger than for pure P. This reflects the

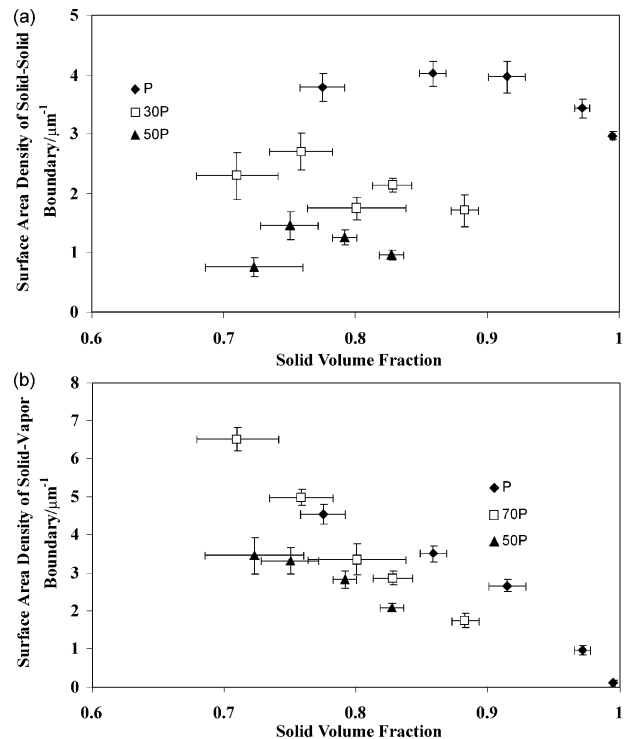


Fig. 3. (a) The effect of the fraction of powder A on the evolution of the surface area density of solid–solid interface as a function of solid volume fraction. (b) The effect of the fraction of powder A on the evolution of the surface area density of solid–vapor interface as a function of solid volume fraction.

variability between the images caused by the extent of the field of view at the magnification required to image the fine particles. For pure P there is some indication at solid volume fractions above 0.95 that the surface area of solid–solid boundaries decreased due to grain growth. There is also a trend to lower values at higher density for 70%P and a slight peak in S_v^{ss} , although this may not be significant. The evolution of the surface area density of pore boundaries is given in Fig. 3(b). As expected, the values decrease gradually as the solid volume fraction increases. Linear decreases in S_v^{sv} with increasing solid volume fraction have been commonly observed in the sintering of powder metals^{21,22} and ceramics.^{20,23,24} Inspection of Eq. (1) shows that this linear relationship implies that the average pore intercept length remains constant through most of sintering. The addition of the coarse particles does not appear to alter the form of this relationship. At any particular value of the solid volume fraction the surface area density of solid–vapor boundary is highest for pure P and decreases as the fraction of the coarse powder increases. For example, at a solid volume fraction of 0.8 the values of S_v^{sv} are $5.1 \mu\text{m}^{-1}$, $4.8 \mu\text{m}^{-1}$ and $2.6 \mu\text{m}^{-1}$ for pure P, 70%P and 50% P, respectively. This is consistent with the average pore size being larger for increasing additions of the coarser powder.

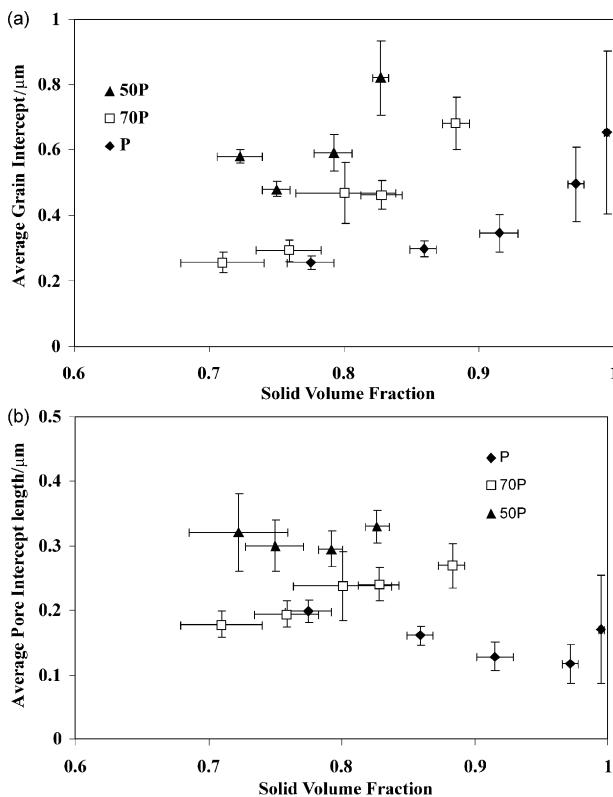


Fig. 4. (a) The effect of the fraction of powder A on the evolution of the average grain intercept length as a function of solid volume fraction. (b) The effect of the fraction of powder A on the evolution of the average pore intercept length as a function of solid volume fraction.

The average grain intercepts were calculated from the results and are summarized in Fig. 4(a). This indicates an apparent effect of the powder additions on the common form of the microstructure map. For pure P the average grain intercept at a solid volume fraction of 0.8 was $0.26 \mu\text{m}$ and remains relatively constant until a solid volume fraction of 0.9 is reached when the grain size increases more rapidly. The average grain intercept for 70%P at a solid volume fraction of 0.8 is $0.38 \mu\text{m}$ and increases relatively rapidly to a value of $0.66 \mu\text{m}$ after 30 h when the solid volume fraction was 0.87. The 50%P samples had a much larger grain size at any value of solid volume fraction. However, the trend is not as clear due to the larger 95% confidence intervals for 50%P. Fig. 4(b) shows the variation in average pore intercept length with solid volume fraction. There are some weak trends such as an increase in pore intercept with density for 70%P. However these trends may not be significant. Collectively, the average values of the pore intercept lengths of the powder mixtures increases as the fraction of coarse powder increases ranging from 0.16 to $0.22 \mu\text{m}$ and $0.35 \mu\text{m}$ for P, 70%P and 50%P, respectively.

4. Discussion

The effect of the mixing on green density was as expected from previous studies.⁵ Increasing the volume fraction of large dense particles reduces the volume occupied by the finer powder particles and the interstices between them and thereby increases green density. This continues for bimodal powders until about 70% coarse particles when the packing of the large particles is thought to dominate with the fine particles fitting in the interstices between them. Further addition of coarse particles causes a decrease in the green density. This may be reflected in the slight decrease in the green density from 30%P to pure A.

The results of the sintering and microstructural study suggest that the large particles slow densification. The effect on densification may reflect an effect of a percolating network of large particles that retards the densification of the matrix as proposed by previous studies.^{13,16} The most pronounced effect on the microstructure is the effect of the coarse particle additions on the density of solid–solid boundaries that develop in the early stages of densification at densities below those examined here, leading to the observed plateaus. This was not unexpected since the larger particles would lower the amount of grain boundary that forms in densification and may also be expected to drive coarsening throughout densification. There is however, an important observation concerning the effect of the mixing on the coarsening of the grains during intermediate stage densification. This is shown in the evolution of the average grain intercept length in Fig. 4(a). When plotted as a function of solid volume fraction, the additions of

coarse powder appear to cause enhanced coarsening at lower densities resulting in an increase of the average grain intercept which could easily be interpreted as the effect of mixing on coarsening behavior. Importantly, when the average grain intercepts for pure P and 70% P are plotted as a function on sintering time (Fig. 5) they collapse onto a common trajectory which suggests that while the addition of the coarse powder did affect densification kinetics it did not affect the kinetics of grain coarsening in these samples. The 50% samples show larger average grain sizes especially at the longer sintering times, although the difference is not as great as when plotted against solid volume fraction. It is thought that the population of fine grains still dominated the average grain intercept in the 70%P samples whereas the presence of more large grains in the 50% sample increases the average intercept length and may drive coarsening at the longer sintering times. The large grains do appear to affect the fine grains to which they are coordinated. The role of the large grain in coarsening can be seen by comparing the micrographs in Fig. 6. Fig. 6(a) shows the microstructure of powder P sintered for 0.2 h with a solid volume fraction of 0.82. The grain size distribution is relatively narrow and the grain boundaries are relatively smooth showing little evidence of the coarsening affecting the fine grains coordinated to larger grains in the mixtures. In Fig. 6(b) the curvilinear boundaries of the large particles are thought to result from smaller surrounding grains that have been consumed by coarsening, breaking the necks they had previously formed with the surrounding matrix leaving larger pore channels adjacent to the large particles. The latter point may be responsible, in part, for the higher average pore intercept length in the mixtures Fig. 4(b). Such a coarsening mechanism will only affect the average grain size when a relatively large number fraction of the fine particles are in contact with the coarse particles. Fig. 7(a) shows 70%P after 30 h of sintering. The growth of the fine grains of the matrix is thought to be largely unaffected by the presence of the coarse grains. This could explain why the average grain intercept length in P and

70%P are the same at any particular sintering time. However, the implication is that coarsening will play a very important role in situations where a relatively small fraction of fine particles is used to bond large particles as in the suggested microstructural design for porous ceramic matrix composites. This will lead to a higher incidence of the situation illustrated by Fig. 7(b) where adjacent large particles are bonded by a few smaller particles. These fine particles could be consumed by the observed coarsening mechanism and the density of particle contacts that contribute to the mechanical integrity of the porous matrix would be reduced. In this respect the use of alumina for both the coarse and fine particle fractions could be detrimental if the material is to spend extended periods of time at high temperature.

The interplay between coarsening and densification in porous ceramics has been studied in several systems.^{25–27} These early studies, which used relatively high temperatures, observed substantial grain growth during intermediate stage sintering at densities less than 60%.

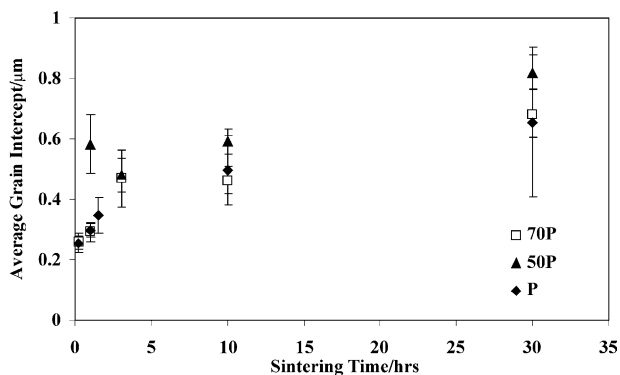
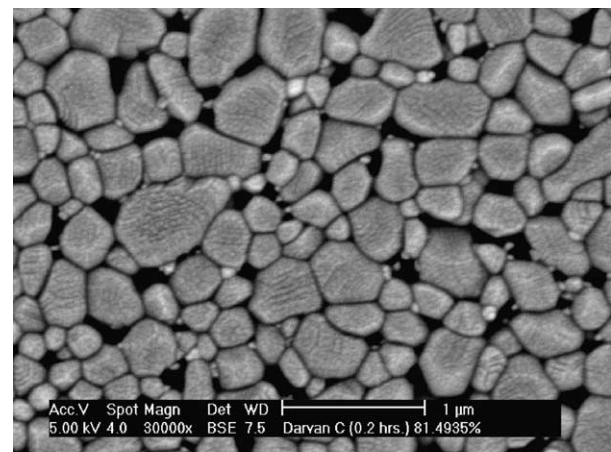
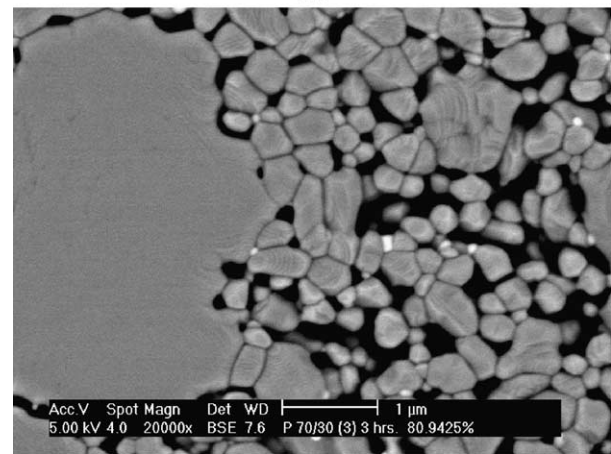


Fig. 5. The evolution of average grain intercept length with sintering time for P, 70%P and 50%P.



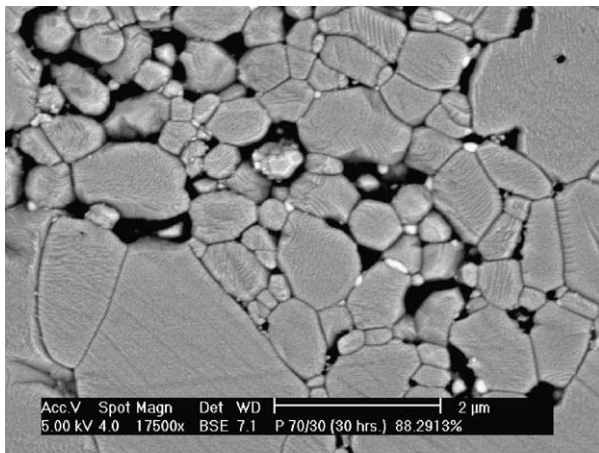
(a)



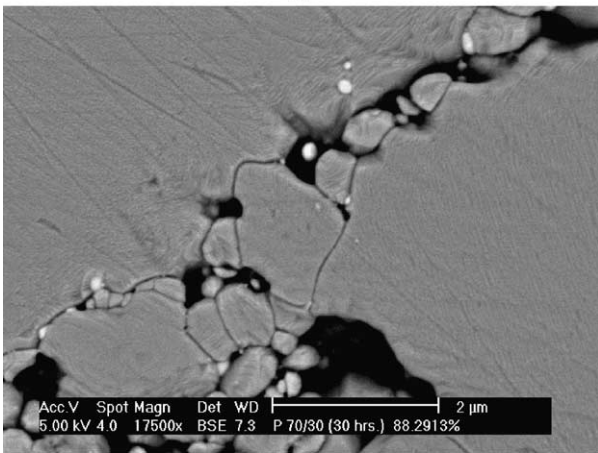
(b)

Fig. 6. (a) SEM image of a sample made from powder P fired for 0.2 h resulting a solid volume fraction of 0.82. (b) SEM image of one of the large grains in a sample containing 70%P sintered for 3 h. The curvilinear boundaries suggest that the coordinating small particles are being consumed by coarsening.

Greskovich and Lay²⁸ concluded that surface diffusion could be responsible for coarsening of structures in which large particles are in contact with relatively few small particles. In contrast, highly coordinated grains were not expected to coarsen. The idea was later used by Cameron and Raj²⁴ who carefully prepared centrifugal cast samples from fine alumina powders which were isothermally sintered at 1550 °C. These samples showed little grain growth in intermediate stage sintering. This was explained using the ideas of Greskovich and Lay²⁸ in that the authors suggested that the colloidal processing of powders with a relatively narrow particle size distribution produced uniform green microstructures and largely avoided the circumstances in which particles of differing size were in contact and yet poorly coordinated. Grain growth was thus delayed until final stage sintering, at which point the elimination of voids allows the grain boundaries to move in response to their curvature. A similar argument can be applied to the behavior in the present study. The samples of pure P contained a relatively narrow size distribution of particles in more spatially uniform green microstructures.



(a)



(b)

Fig. 7. (a) SEM image of 70%P sintered for 30 h. (b) SEM image of 70%P sintered for 30 h showing small grains separating adjacent large grains.

Therefore grain coarsening of the type postulated by Greskovich and Lay²⁸ may not be significant. When large particles were added to the microstructure, the size difference is available to drive grain coarsening when the small particles coordinated to them form necks. It is thought that further neck growth to the large dense particles causes the small coordinating grains to “de-sinter”¹³ from the surrounding matrix which is compelled to shrink away from the dense coarse particle if there is a percolating network. The reduction in the coordination number of the fine particles by “de-sintering” then allows the fine particles in contact with the large particle to be consumed by coarsening in the manner proposed by Greskovich and Lay.²⁸ This is reflected in the curvilinear boundaries of the coarse particle in Fig. 6(b). However, this mechanism appears not to be significant enough to affect the coarsening kinetics in the 70%P samples, as reflected in the average grain intercept, because of the relatively low number density of coarse particles. In contrast there is a significant effect on the densification kinetics resulting in the apparent difference in coarsening behavior when average grain intercept is plotted as a function of solid volume fraction. When the fine powder fraction is decreased to 50%P a much larger fraction of the fine powder particles are in contact with coarse particles and the coarsening mechanism described above is thought to effect the average grain intercept to the extent that there is now a difference in the plot of average grain intercept against sintering time, especially at longer times.

5. Conclusion

This work investigated the microstructural evolution of alumina when coarse powder particles with a relatively wide particle size distribution were added to a fine alumina powder. As expected, the addition of the coarse particles increased the green density but severely decreased the consequent densification. Examination of the microstructural evolution showed that the presence of large particles increased the grain size when plotted against solid volume fraction in a conventional microstructure map. However, when the average grain intercept was plotted as a function of time the results for P and 70%P showed no difference, suggesting that enhanced coarsening did not occur for the majority of the fine grains in intermediate sintering and was not sufficient to affect the average grain intercept length. Qualitative observations on the other hand, showed that coarsening did occur in which the coarse particles consumed coordinating fine particles thereby enlarging adjacent pores. This suggests that coarsening in microstructural evolution for powder mixtures may be more deleterious when coarse particles are bonded together with a relatively small fraction of fine particles.

Acknowledgements

The authors would like to thank the National Science Foundation for funding through grant CMS 970062.

References

1. Ting, J. M. and Lin, R. Y., Effect of particle size distribution on sintering: Part II sintering of alumina. *J. Mat. Sci.*, 1995, **30**, 2382–2389.
2. Yeh, T. S. and Sacks, M. D., Effect of particle size distribution on the sintering of alumina. *J. Am. Ceram. Soc.*, 1988, **71**, C484–C487.
3. Shiau, F. S., Fang, T. T. and Leu, T. H., Effect of particle-size distribution on the microstructural evolution in the intermediate stage of sintering. *J. Am. Ceram. Soc.*, 1997, **80**, 286–290.
4. Chappell, J. S., Ring, T. A. and Birchall, J. D., Particle size distribution effects on sintering rates. *J. Appl. Phys.*, 1986, **60**, 383–391.
5. Messing, G. L. and Onoda, G. Y., Inhomogeneity-packing density relations in binary powder. *J. Am. Ceram. Soc.*, 1978, **61**, 1–5.
6. O'Hara, M. J. and Cutler, I. B., Sintering kinetics of binary mixtures of alumina powders. *Proc. Brit. Ceram. Soc.*, 1969, **12**, 145–154.
7. Smith, J. P. and Messing, G. L., Sintering of bimodally distributed alumina powders. *J. Am. Ceram. Soc.*, 1984, **67**, 238–242.
8. Raj, R. and Bordia, R. K., Sintering of bimodal powder compacts. *Acta Metall.*, 1984, **32**, 1003–1019.
9. Scherer, G. W., Sintering with rigid inclusions. *J. Am. Ceram. Soc.*, 1987, **70**, 719–725.
10. Lange, F. F. and Metcalf, M., Processing related fracture origins: II agglomerate motion and crack-like internal surfaces caused by differential sintering. *J. Am. Ceram. Soc.*, 1983, **66**, 398–406.
11. DeJonghe, L. C., Rahaman, M. N. and Hseuh, C. H., Transient stresses in bimodal compacts. *Acta Metall.*, 1986, **34**, 1467–1471.
12. Bordia, R. K. and Raj, R., Sintering of TiO_2 - Al_2O_3 composites: a model experimental investigation. *J. Am. Ceram. Soc.*, 1988, **71**, 302–310.
13. Sudre, O. and Lange, F. F., Effect of inclusions on densification: I, microstructural development in an Al_2O_3 matrix containing a high volume fraction of ZrO_2 inclusions. *J. Am. Ceram. Soc.*, 1992, **75**, 519–524.
14. Evans, A. G., Considerations of inhomogeneity effects in sintering. *J. Am. Ceram. Soc.*, 1982, **65**, 497–501.
15. Tuan, W. H., Gilbert, E. and Brook, R. J., Sintering of heterogeneous ceramic compacts, Part I Al_2O_3 - Al_2O_3 . *J. Mat. Sci.*, 1989, **24**, 1062–1068.
16. Fan, C. L. and Rahaman, M. N., Factors controlling the sintering of ceramic particulate composites: I, conventional processing. *J. Am. Ceram. Soc.*, 1992, **75**, 2056–2065.
17. Levi, C. G., Yang, J. Y., Dalgleish, B. J., Zok, F. W. and Evans, A. G., Processing and performance of an all-oxide ceramic composite. *J. Am. Ceram. Soc.*, 1998, **81**, 2077–2086.
18. Robinson, R. C. and Smialek, J. L., SiC recession caused by SiO_2 scale volatility under combustion conditions: I experimental results and empirical model. *J. Am. Ceram. Soc.*, 2000, **82**, 1817–1825.
19. Steel, S. G., Zawada, L. P. and Mall, S., Fatigue behavior of a NEXTEL 720/alumina composite at room and elevated temperature. *Ceram. Eng. & Sci. Proc.*, 2001, **22**, 695–702.
20. Lehigh, M. D. and Nettleship, I., Microstructural evolution of porous alumina. *Mat. Res. Soc. Symp. Proc.*, 1995, **371**, 315–320.
21. Aigeltinger, E. H. and DeHoff, R. T., Quantitative determination of topological and metric properties during the sintering of copper. *Metall. Trans.*, 1975, **6A**, 1853–1862.
22. Aigeltinger, E. H. and Exner, H. E., Stereological characterization of the interaction between interfaces and its application to the sintering process. *Metall. Trans.*, 1977, **8A**, 421–424.
23. Shaw, N. J. and Brook, R. J., Structure and grain coarsening during the sintering of alumina. *J. Am. Ceram. Soc.*, 1986, **69**, 107–110.
24. Cameron, C. P. and Raj, R., Grain-growth transition during sintering of colloiddally prepared alumina powder compacts. *J. Am. Ceram. Soc.*, 1988, **71**, 1031–1035.
25. Gupta, T. K. and Coble, R. L., Sintering of ZnO: I densification and grain growth. *J. Am. Ceram. Soc.*, 1968, **51**, 512–525.
26. Clare, T. E., Sintering kinetics of beryllia. *J. Am. Ceram. Soc.*, 1965, **49**, 159–165.
27. Gupta, T. K., Possible correlation between density and grain size during sintering. *J. Am. Ceram. Soc.*, 1972, **55**, 276–277.
28. Greskovich, C. and Lay, L. W., Grain growth in very porous Al_2O_3 compacts. *J. Am. Ceram. Soc.*, 1972, **55**, 142–146.